

Figure 1. Mass spectrum of $\text{Cu}^+(\text{NH}_3)_n$ clusters at 7-torr pressure of ammonia. The ^{63}Cu and ^{65}Cu isotopes are evident in each cluster peak.

transition-metal ions (copper) has been the use of laser vaporization of the metal to produce ions.² These techniques are less than ideal, the first due to the complicating presence of unwanted fragment ions, and the second due to the excess kinetic energy of laser-generated ions.

We report that it is possible to generate transition-metal ions by thermionic emission and that we are currently using Cu^+ and Ag^+ filaments in our laboratory for studies of ion clustering with water and ammonia as ligands. The general method we use for the preparation of thermionic emission filaments has been described earlier in this journal.³ In the case of the Cu^+ and Ag^+ filaments described above, the procedure is particularly dependent on the use of high-purity starting materials⁴ followed by several hours of operation during which alkali metal ion impurities are baked out. The resulting filaments have only trace alkali metal impurities, and we have found them to be suitable for several weeks of almost continuous use.

The solvation structure and coordination of ligands about ions are areas of particular interest in our research program. Burnier et al.² have suggested that no distinct inner- and outer-coordination spheres are apparent in the ΔH values of alkali metal ions clustered by ligands such as H_2O , NH_3 , and CH_3CN . We point out work carried out in our laboratory on the clustering of ammonia about alkali metal ions^{3,5} and, in particular, evidence that well-defined "coordination shells" may exist for the Li^+ and Na^+ systems.³ Other evidence of possible "coordination" in the gas phase is shown in ΔH plots of water about Sr^+ ion⁶ and NH_4^+ ion⁷ which suggest that they are 8- and 4-coordinate, respectively. It is likely that the apparent "coordination" in the gas phase for some systems reflects a special "fit" of ligands about the central ion to form a highly ordered structure. This is unlike the case for many ion clusters where less ordered structures similar to those obtained in Monte Carlo calculations⁸ are probable.

Studies of clustering about transition-metal ions should provide particularly useful information relevant to coordination phenomena since many coordination complexes are known to exist in solution.

This is because in gas-phase clustering studies the binding of additional ligands, beyond those of the known coordination complex in solution, can be examined. For example, the mass spectrum in Figure 1 shows the Cu^+ ion with 3, 4, and 5 ammonia ligands whereas in solution the coordination complex $\text{Cu}^+(\text{NH}_3)_2$ occurs. It has been suggested in an earlier study that the third ammonia ligand has an intrinsically weak interaction.² Our results show that while the third, fourth, and fifth ammonia ligands in $\text{Cu}^+(\text{NH}_3)_n$ bind less strongly than the corresponding water ligands in $\text{Cu}^+(\text{H}_2\text{O})_n$, they each have binding energies in excess of 10 kcal/mol. In particular, equilibrium measurements have been used to determine requisite binding energies for the reactions of M^+ ($\text{M} = \text{Cu}, \text{Ag}$) with ammonia, represented by eq 1 ($n = 2-4$).



The standard enthalpy values for copper are 14.0, 12.8, and 12.8 kcal/mol, respectively, while those for silver are 14.6, 13.0, and 12.8 kcal/mol. This demonstrates that ligands beyond the "coordination" complex (with two ligands) still have significant binding energies (even though binding in the coordination complexes is well in excess of 30 kcal/mol). The observed $\text{Cu}^+(\text{NH}_3)_2$ species in solution is probably due to preferential bonding of the ion to solvent beyond the second ligand, rather than to an intrinsic inability to bind additional ligands.

Gas-phase clustering about transition-metal ions is a promising new area of chemistry which should offer important information and insights relevant to both the study of coordination complexes and solvation phenomena.

Acknowledgment. Support of the Atmospheric Sciences Section of the National Science Foundation under Grant ATM 79-13801 is gratefully acknowledged. The Cooperative Institute for Research in Environmental Sciences is jointly sponsored by the University of Colorado and NOAA.

Paul M. Holland, A. W. Castleman, Jr.*

Department of Chemistry and Chemical Physics Laboratory
University of Colorado, Boulder, Colorado 80309

Received April 18, 1980

Fluxional Behavior of $[\text{Rh}_{14}(\text{CO})_{25}\text{H}_{4-n}]^{n-}$ ($n = 3$ and 4)

Sir:

The carbonyl cluster anions $[\text{Rh}_{13}(\text{CO})_{24}\text{H}_{5-x}]^{x-}$ ($x = 3$ and 2) exhibit carbonyl migration on the outside and H migration on the inside of the hexagonal close-packed metal skeleton;¹ both migrations necessitate the involvement of all twelve outer rhodium atoms. Recent work² has shown that the activation energies for carbonyl and H migrations are similar, and it thus seems probable that the migratory motions of both ligands are interrelated. We now report on the fluxional behavior of $[\text{Rh}_{14}(\text{CO})_{25}\text{H}_{4-n}]^{n-}$ ($n = 4$ and 3); the monohydride provides a second example of interstitial H migration, but in this case, the hydrogen migrates to rhodium atoms which are *not* involved in carbonyl rearrangements.

The X-ray structures of $[\text{Rh}_{14}(\text{CO})_{25}]^{4-}$ and $[\text{Rh}_{14}(\text{CO})_{25}\text{H}]^{3-}$ are very similar^{3,4} and are shown schematically in Figure 1. A well-resolved ^{13}C NMR spectrum of $[\text{Rh}_{14}(\text{CO})_{25}]^{4-}$ in EtCN was obtained on lowering the temperature to -60°C . This is shown in Figure 2e together with the assignments which have been established by ^{13}C - ^{103}Rh NMR studies. Thus, irradiation at 3.156847 MHz [δ (^{103}Rh) -1001^5] collapses only the quintet at

(1) See, for instance: Allison, J.; Ridge, D. P. *J. Am. Chem. Soc.* **1979**, *101*, 4998. Foster, M. S.; Beauchamp, J. L. *Ibid.* **1975**, *97*, 4808.

(2) Burnier, R. C.; Carlin, T. J.; Reents, W. D., Jr.; Cody, R. B.; Lengel, R. K.; Freiser, B. S. *J. Am. Chem. Soc.* **1979**, *101*, 7127.

(3) Castleman, A. W., Jr.; Holland, P. M.; Lindsay, D. M.; Peterson, K. I. *J. Am. Chem. Soc.* **1978**, *100*, 6039.

(4) For example, we use Baker "Ultrax" Al_2O_3 and reagent-grade silicic acid (in place of SiO_2) together with the nitrate of the metal ion desired.

(5) Castleman, A. W., Jr. *Chem. Phys. Lett.* **1978**, *53*, 560.

(6) Tang, I. N.; Castleman, A. W., Jr. *J. Chem. Phys.* **1975**, *62*, 4576.

(7) Payzant, J. D.; Cunningham, A. J.; Kebarle, P. *Can. J. Chem.* **1973**, *51*, 3242.

(8) Clementi, E. "Determination of Liquid Water Structure Coordination Numbers for Ions and Solvation for Biological Molecules", Springer-Verlag: Heidelberg, 1976; Vol. 2, pp 1-107.

(1) S. Martinengo, B. T. Heaton, R. J. Goodfellow, and P. Chini, *J. Chem. Soc., Chem. Commun.*, **39** (1977)

(2) B. T. Heaton, S. Martinengo, P. Chini, unpublished results.

(3) S. Martinengo, G. Ciani, A. Sironi, and P. Chini, *J. Am. Chem. Soc.*, **100**, 7096 (1978)

(4) G. Ciani, A. Sironi, and S. Martinengo, *J. Organomet. Chem.*, **192**, C42 (1980).

(5) For δ (^{103}Rh), $\delta \text{O} = 3.16$ MHz at a magnetic field such that the protons in Me_4Si resonate at exactly 100 MHz; shifts to high frequency are positive.

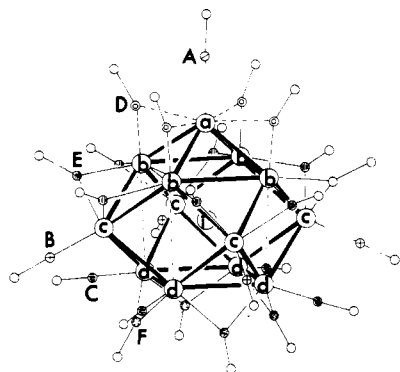


Figure 1. Schematic structure of $[\text{Rh}_{14}(\text{CO})_{25}\text{H}_{4-n}]^{n-}$ ($n = 4$ and 3).^{3,4}

Table I. ^{13}C and ^{103}Rh NMR Data for $[\text{Rh}_{14}(\text{CO})_{25}\text{H}_{4-n}]^{n-}$ ($n = 4^a$ and 3^b)

	$n = 4$	$n = 3$
δ (Rh_a)	+200	+136
δ (Rh_b)	-939	-840
δ (Rh_c)	+320	+231
δ (Rh_d)	-1001	-973
δ (Rh_i)	<i>c</i>	+5936
δ (CO_A)	192.7	185.7
J ($\text{Rh}_a\text{-CO}_A$), Hz	102	101
δ (CO_B)	186.2	181.2
J ($\text{Rh}_c\text{-CO}_B$), Hz	89	91.5
δ (CO_C/CO_F)	208.5	202
" J ($\text{Rh}_d\text{-CO}_C/\text{CO}_F$)", Hz	21.5	<i>d</i>
δ (CO_D)	232.9	219.0
J ($\text{Rh}_a\text{-CO}_D$), Hz	17	15
J ($\text{Rh}_b\text{-CO}_D$), Hz	62	61
δ (CO_E)	250.5	237.0
J ($\text{Rh}_b\text{-CO}_E$), Hz	44	44
J ($\text{Rh}_c\text{-CO}_E$), Hz	44	37

^a At -60°C . ^b At -80°C . ^c Could not be obtained from ^{13}C - ^{103}Rh measurements. ^d The quintet is not well-resolved at this temperature.

δ 208.5 (Figure 2d), allowing these resonances to be assigned to edge/terminal (CO_C/CO_F) exchange around the (Rh_4)₄ square face; other ^{103}Rh -decoupling experiments (Figure 2a-c) produce results which are in accord with the solid-state structure. Similar behavior is found for $[\text{Rh}_{14}(\text{CO})_{25}\text{H}]^{3-}$ at -80°C , and the ^{13}C and ^{103}Rh NMR data for $[\text{Rh}_{14}(\text{CO})_{25}\text{H}_{4-n}]^{n-}$ ($n = 4$ and 3) are summarized in Table I.

The ^1H NMR spectrum of $[\text{Rh}_{14}(\text{CO})_{25}\text{H}]^{3-}$ at -80°C is a broad, ill-defined resonance, δ (^1H) -31.3 . ^1H - ^{103}Rh INDOR measurements readily locate the interstitial rhodium atom, Rh_i , (Table I), and a combination of INDOR and specific spin-decoupling experiments have located Rh_b , Rh_c , and Rh_d .⁶ When Rh_b and Rh_d are simultaneously decoupled, the doublet due to Rh_i [J (Rh_i , H) = 16.5 Hz] is clearly visible, but triple-resonance experiments failed to show the multiplet structures due to the other rhodium atoms. However, it is clear that the couplings to these peripheral metal atoms are much smaller than to Rh_i , cf. $[\text{Rh}_{13}(\text{CO})_{24}\text{H}_{5-x}]^{x-}$ ($x = 3$ and 2),¹ which, combined with the fourfold symmetry implied by the ^{13}C spectrum, strongly support H migration within the Rh_b , Rh_c , and Rh_d cage. Since at this temperature only CO_C and CO_F on Rh_d are migrating, we conclude that carbonyl and hydride migrations in $[\text{Rh}_{14}(\text{CO})_{25}\text{H}]^{3-}$ occur independently.

The chemical shifts of the majority of other interstitial atoms (^{13}C , ^{31}P , ^{103}Rh , and sometimes ^1H) are all at high frequency⁷ in a region normally associated with positive oxidation states of these elements, and δ (Rh_i) in $[\text{Rh}_{14}(\text{CO})_{25}\text{H}]^{3-}$ is in keeping with

(6) The values of δ (^{103}Rh) obtained by ^1H - ^{103}Rh measurements are all within 5 ppm of those obtained by ^{13}C - ^{103}Rh . It was not possible to locate Rh_a by ^1H - ^{103}Rh INDOR because of the small perturbation resulting from the small coupling to this unique rhodium atom.

(7) P. Chini, *J. Organomet. Chem.*, in press.

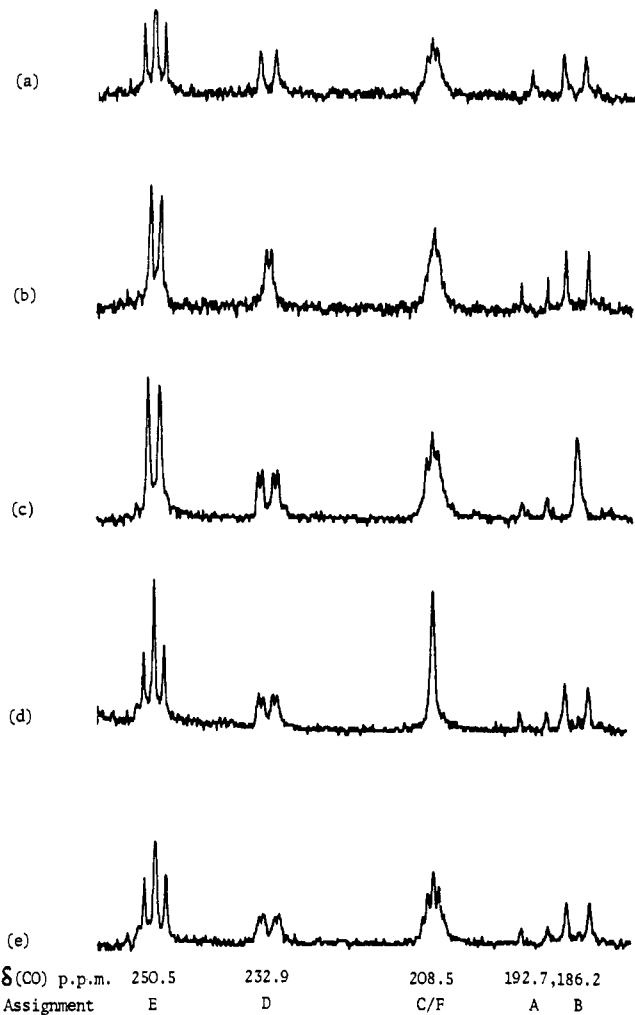


Figure 2. ^{13}C - ^{103}Rh -decoupled (a-d) and ^{13}C NMR (e) spectra of $(\text{NEt}_4)_4[\text{Rh}_{14}(\text{CO})_{25}]$ (ca. 40% ^{13}C) in EtCN at -60°C ; decoupling at (a) 3.160643 MHz [δ (Rh_a) +200]; (b) 3.157043 MHz [δ (Rh_b) -939]; (c) 3.161022 MHz [δ (Rh_c) +320]; (d) 3.156847 MHz [δ (Rh_d) -1001].

these observations. The rather large alternation in δ (^{103}Rh) between layers on the C_4 axis in $[\text{Rh}_{14}(\text{CO})_{25}\text{H}_{4-n}]^{n-}$ ($n = 4$ and 3) is similar to that found along the C_3 axis in $[\text{Rh}_7(\text{CO})_{16}]^{3-8}$ and may also reflect differences in charge distribution.⁹ Finally, it should be noted that although similar localized carbonyl exchanges have been observed for $[\text{Rh}_{14}(\text{CO})_{25}\text{H}_{4-n}]^{n-}$ ($n = 4$ and 3) and $[\text{Rh}_7(\text{CO})_{16}]^{3-8}$, the exchange occurs on rhodium atoms

(8) C. Brown, B. T. Heaton, L. Longhetti, and D. O. Smith, *J. Organomet. Chem.*, **169**, 309 (1979).

(9) The metal chemical shifts of mononuclear cobalt and rhodium complexes move to lower frequency with decreasing oxidation state.^{10,11} For the isoelectronic series of clusters $[\text{Rh}_4(\text{CO})_{12}]$, $[\text{Rh}_4(\text{CO})_{11}(\text{COOMe})^-]$, and $[\text{Rh}_4(\text{CO})_{11}]^{2-}$, δ (^{103}Rh), when measured under fast carbonyl-exchange conditions, is -426 (at $+60^\circ\text{C}$); -494 and +202 (Rh-COOMe) (at -30°C); and -431 (at -30°C), respectively. Apart from the unique Rh-COOMe resonance, there is little variation in δ (^{103}Rh) since the increasing charge is delocalized onto the carbonyl ligands as evidenced by the progressive high-frequency shift of δ (^{13}C), 190.5, 201.8, and 222.8, respectively. However, the high-frequency shift of the unique rhodium in $[\text{Rh}_4(\text{CO})_{11}(\text{COOMe})^-]$ is in keeping with an expected more positive metal atom. A similar explanation could account for the apical cobalt resonance in $\text{Co}_4(\text{CO})_{12}$ being at higher frequency than the basal cobalt resonances¹² since recent CNDO calculations¹³ show the apical cobalt to be significantly more positive than the basal cobalt atoms.

(10) R. J. Goodfellow, "N.M.R. and the Periodic Table", Academic Press, New York, 1978, p 225.

(11) C. Brown, B. T. Heaton, L. Longhetti, W. T. Povey, and D. O. Smith, *J. Organomet. Chem.*, **192**, 93 (1980).

(12) M. A. Cohen, D. R. Kidd, and T. L. Brown, *J. Am. Chem. Soc.*, **97**, 4408 (1975).

(13) H. J. Freund and G. Hohlneicher, *Theor. Chim. Acta*, **51**, 145 (1979).

which have low- and high-resonance frequencies, respectively; in both cases, the dominant factor in determining carbonyl fluxionality appears to be steric strain, which results from carbonyls on adjacent layers being eclipsed. This strain is relieved by carbonyl migration on an *outer* Rh₄ or Rh₃ face, respectively.

Acknowledgment. We thank the S.R.C. for a research fellowship (to L.S.) and also CNR/British Council for a grant (to P.C. and B.T.H.).

† Deceased.

Brian T. Heaton,* Charles Brown, David O. Smith
Luisella Strona

Chemical Laboratory, University of Kent
Canterbury, CT2 7NH, England

Robin J. Goodfellow

Inorganic Chemistry Department
University of Bristol, BS8 1TS, England

Paolo Chini†

Istituto di Chimica Generale dell' Università
20133-Milano, Italy

Secondo Martinengo

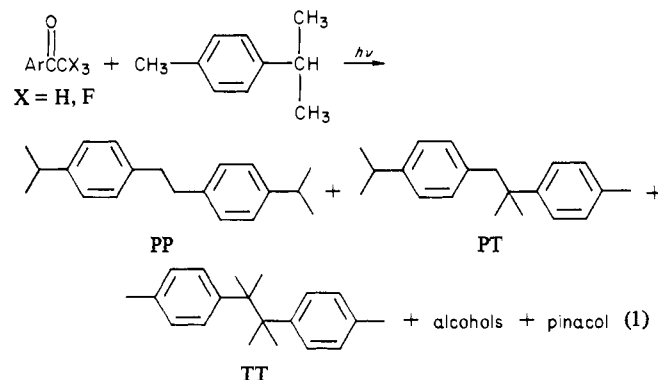
Centro del C.N.R. sui bassi stati di ossidazione
20133-Milano, Italy

Received June 2, 1980

Varying Selectivities of Triplet Ketones toward *p*-Cymene: A Measure of the Extent of Charge Transfer in Triplet Exciplexes

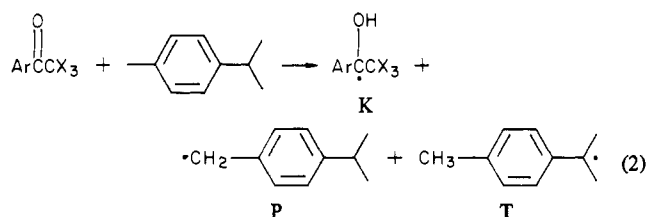
Sir:

We recently reported that triplet α -trifluoroacetophenone (AF₃) attacks *p*-cymene to yield primary and tertiary benzylic radicals in a 3.4:1 ratio, in contrast to the 1:2.8 P/T ratio observed with acetophenone (AH₃) itself (eq 1).¹ We ascribed the difference



to the fact that hydrogen abstraction by triplet AF₃ proceeds via an exciplex intermediate² with substantial positive charge on the cymene. The 3.4:1 ratio could indicate an almost total lack of selectivity in exciplex H transfer, since it nearly equals the ratio of available benzylic hydrogens. We now find that the P/T radical ratio varies as a function of ring substitution on both AF₃ and AH₃. The apparently random ratio with AF₃ itself is just coincidental. More importantly, the P/T ratio serves as a unique probe of the extent of charge transfer in an exciplex.

Degassed benzene solutions containing various substituted ketones (0.05 M) and 0.5 M *p*-cymene were irradiated at 313 nm until 2–15% of the ketone had reacted (eq 2). The relative amounts of the three substituted bibenzyl radical coupling products were determined by gas chromatographic analysis.¹ The measured



ratios are listed in Table I, as are the P/T radical ratios which would account for the product distributions.³

For both AF₃ and AH₃, electron-withdrawing substituents increase the P/T ratio, and electron-donating substituents decrease it, with a given substituent having roughly twice as large an effect on AF₃ as on AH₃. The effects can be related qualitatively to the degree of positive charge on the cymene in the exciplex formed with it as donor to triplet ketone, if it is accepted that high P/T selectivity results from positive charge density on the cymene.¹ There are now many examples of kinetic acidity effects dominating exciplex decay.⁴ Unfortunately, as discussed earlier,¹ it is not known what P/T ratio would result from free *p*-cymene radical cation, so we cannot yet put our results on a quantitative basis.

Table I also includes some rate constants for interactions of the triplet ketones with *toluene*, which we have reported elsewhere.⁵ For AF₃, there is a fourfold variation in P/T over a 10⁴-fold variation in bimolecular rate constants for exciplex formation.⁶ Figure 1 compares how *k* and P/T vary with triplet reduction potential. There have been suggestions that the slopes of plots of log *k* vs. ΔG for electron transfer reveal the extent of electron transfer during exciplex formation.^{2,7} For example, in Figure 1, the slope of log *k* vs. E_{red}^* is only 0.40/room temperature.⁵ Slopes lower than 1/room temperature definitely establish that the reaction does not involve complete one-electron transfer with the formation of metastable radical ions.⁸ However, it might be expected that the amount of charge separation in exciplexes formed from a common donor should vary with the reduction potential of the acceptor. Our present results, as plotted in Figure 1, provide the first experimental corroboration of this chemical intuition and indicate that linear plots of log *k* vs. ΔG do not demonstrate a constant degree of charge separation for all pairs plotted (e.g., 40% in the AF₃-*toluene* series).

Irradiation of 0.1 M di-*tert*-butyl peroxide in 0.6 M *p*-cymene produces the three bibenzyls in proportions which indicate a P/T ratio of 1:2.7, the same observed in the photoreduction of AH₃. This fact, together with a k_H/k_D value of 3.3 observed in the quenching of acetophenone phosphorescence by *toluene* and *toluene-d*₈,^{9,10} might suggest that triplet AH₃ reacts with *toluene* by direct hydrogen atom abstraction. However, the substituent effects now observed on P/T ratios from AH₃ indicate that the photoreduction of AH₃ by alkylbenzenes generates partial positive charge on the alkylbenzene during hydrogen transfer. Given that the actual rate constant for quenching of triplet ketones by *toluene* correlates with *toluene*'s oxidation potential,^{7a} our present results suggest that the photoreduction of AH₃ by alkylbenzenes proceeds from a reversibly formed exciplex with a small amount of CT, possibly in competition with direct hydrogen atom abstraction.

(3) When all three hydrocarbons were measurable, $P/T = (PP/TT)^{1/2} = (2PP + PT)/(PT + 2TT)$. When either PP or TT was present in too small an amount to be measured accurately, or when other product peaks interfered with GC analysis, $P/T = 2PP/PT = PT/2TT$. These equations reflect the statistical coupling behavior of P and T radicals and the fact that the two alcohol products containing P and T obtained from AF₃ display the same P/T ratio as measured from the hydrocarbon yields.¹

(4) (a) Cohen, S. G.; Stein, N. M. *J. Am. Chem. Soc.* **1971**, *93*, 6542. (b) Lewis, F. D.; Tong-Ing, H. *Ibid.* **1980**, *102*, 1751.

(5) Wagner, P. J.; Lam, H. M. *J. Am. Chem. Soc.* **1980**, *102*, 4167.

(6) We are currently checking the assumption that the *k* values measure exciplex formation for the less reactive AF₃'s just as for AF₃ itself.²

(7) (a) Guttenplan, J. B.; Cohen, S. G. *J. Am. Chem. Soc.* **1972**, *94*, 4040.

(b) Loutfy, R. O.; Dogra, S. K.; Yip, R. W. *Can. J. Chem.* **1979**, *57*, 342.

(8) Scandola, F.; Balzani, V. *J. Am. Chem. Soc.* **1979**, *101*, 6140.

(9) Mueller, W. H., unpublished results.

(10) The primary isotope effect measured for *tert*-butoxy radicals is 5.25: Walling, C.; McGuinness, J. *J. Am. Chem. Soc.* **1969**, *91*, 2053.

(1) Wagner, P. J.; Puchalski, A. E. *J. Am. Chem. Soc.* **1978**, *100*, 5948.
(2) Wagner, P. J.; Leavitt, R. A. *J. Am. Chem. Soc.* **1973**, *95*, 3669.